

Theoretical approach of OLED thiophene and 1, 3, 4-oxadiazol ligand: Insight from DFT and TD-DFT

Souhila Bekhbek^{1,2}, Nadia Ouddai^{2*} and Rusli Daik³

¹Departement de Chimie, Faculte des Sciences Exactes, Univ Freres Mentouri, Constantine-Algeria

²Laboratoire Chimie des Materiaux et des Vivants: Activite, Reactivite, Univ-Batna1, Algeria

³School of Chemical Sciences & Food Technology, Faculty of Science & Technology,

Universiti Kebangsaan Malaysia, 43600 Bangi, Selangor, Malaysia

*Corresponding author: E-Mail: ouddai_nadia@yahoo.fr

ABSTRACT

We report a theoretical study about the effects of the thiophene and 1, 3, 4-oxadiazol groups on five organic molecules with help of DFT and TD-DFT calculations. By using DFT/B3LYP/6-31G(d, p) to investigate the electronic structures and related properties for studied compounds in ground state, which can be found that the alkyloxy group has no effect on the HOMO-LUMO gap. The lower LUMO energy for BBN₂ and BBN₂F₂ or larger electron affinity (EA), which are also favorable for hole transport. The higher HOMO energy for BHT₂ and BBT₂Br₄ or smaller ionization potential (IP), which are also favorable for electron transport. The maps of electrostatic potential (MEP) for the five diodes, is discussed in term of colors change and ligand groups presence, reactivity indices, showed for BBN₂ and BBN₂F₂ as a strong electrophile. The AIM analysis reveals bonds in compounds belong to closed-shell type interactions, and another side, we used TD-DFT/B3LYP, CPCM/TD-DFT-B3LYP in gas and solvent phase respectively as a quantum methods to investigated the Photophysical properties in excited for thiophene and 1, 3, 4-oxadiazol ligand, absence of solvatochromism in all absorptions spectra. To achieve deep blue emission, with increasing 1, 3, 4-oxadiazol group and achieved the hypsochromic shift. The thiophene group shows the reverse and emits red color.

KEY WORDS: OLED, Reactivity index, Topological analysis, MEP, DFT and TD-DFT.

1. INTRODUCTION

Development of novel electronic donor/acceptor materials is an important topic in the research of (Organic Light Emitting Diodes) compounds. In organic semiconductor; the research of new material on π -conjugated molecules to operate as active materials have become one of the most interesting of chemistry. Since Tang et al, and Friend et al, have been reported of organic light-emitting diode OLED. The thiophene based materials has more interest of research due to the large π conjugation and the good planarity. The 1, 3, 4-oxadiazole groups are highly attractive. Hence, these groups are given excellent charge transport materials. In addition, 1, 3, 4-oxadiazol are increasing electron affinity. We report a theoretical study about the compounds belongs to the family of aryl thiophene compounds to produce polymers, 1,4-Dibromo-2,5-dibutoxybenzene, (BBBr₂), 2,2'-[2,5-Bis (hexyloxy) 1,4-phenylene] dithiophen (BHT₂) and 3,5-Dibromo-2[2,5-dibutoxy-4-(3,5-dibromothiophen-2yl)phenyl] (BBT₂Br₄). In this work we carried out a quantum calculation based on the density functional theory DFT and time dependent TD-DFT, the electronic structures, molecular electrostatic potentials MEP, reactivity indices, topological analysis, absorptions spectra and emission spectra of diodes are discussed and analyzed.

2. METHODS & MATERIALS

Computational details: Density functional theory calculations were carried out using the Gaussian 09W program packages developed by Frisch and coworkers. The Becke's three parameter hybrid functional using the LYP correlation functional (B3LYP), one of the most robust functional of the hybrid family, was herein used for all the calculations, with 6.31G (d, p) basis set. Gaussian output files were visualized by means of GAUSSIAN VIEW 05 software the calculation of the Topological study of electron density, QTAIM analysis were carried out using ADF 2010 program with utilizing the generalized-gradient approximation (GGA) was employed in the geometry optimization by using the Perdew-Burke-Ernzerhof (PBE), the approximation (ZORA).

3. RESULTS AND DISCUSSION

Geometric and electronic properties: The optimized geometries obtained by functional B3LYP with 6.31G(d, p) basis set of the studied molecules, the schematic structures are presented in Fig.1, and the main structurale parameters are summarized in Table.1,2, we can see that our values agree well with the experimental measurement. In BBBr₂, the alkyl chain is found coplanar with the benzene ring; thus confirmed that the molecule is essentially planar, the bond lengths O1-C3, C4-O1 in BBBr₂ and O1-C1, O1-C8 in BHT₂, O2-C8, C10-O2 in BBN₂ and BBN₂F₂; showed insignificant change indicating that the alkyloxy ligand has no effect. In the 1,3,4-oxadiazol compound, we note the presence of a slight effect, the 1,3,4-oxadiazol ligand is twisted relative to the benzene ring, making a dihedral angles O1-C1-C3-C8 0.17° and 0.15° in BBN₂ and BBN₂F₂ respectively. The theoretical electronic property parameters (E_{HOMO}, E_{LUMO} and Gap).Calculated band gaps were in the range of 3.73-5.09eV.The calculated parameters (E_{HOMO}, E_{LUMO}, Gap) of, BHT₂, BBT₂Br₄, BBBr₂,BBN₂ and BBN₂F₂ are (-4.938, -5.426, -5.614, -5.803, -5.962 eV), (-1.212,

-1.653, -0.515, -1.954, -2.170 eV) and (3.73, 3.77, 5.09, 3.85, 3.79 eV), respectively. The calculated band gap E_{gap} of the studied compound increases in the following order $\text{BHT}_2 < \text{BBT}_2\text{Br}_4 < \text{BBN}_2\text{F}_2 < \text{BBN}_2 < \text{BBBr}_2$ indicating, of BBBr_2 the most stable compound, the HOMO/LUMO energies in agreement with their electron donor/acceptor character, allow the HOMO and the LUMO energy levels of the donor and acceptor compounds are very important factors to determine between donor and acceptor. As shown in Fig.2, of BHT_2 and BBT_2Br_4 , the most donor molecules due the HOMO levels are higher than those of BBN_2 , BBN_2F_2 and BBBr_2 . On the other hand, of BBN_2F_2 and BBN_2 the most acceptor compounds, the LUMO of BBN_2F_2 and BBN_2 are lower than those of BHT_2 and BBT_2Br_4 ; it is important to note that the substitution of thiophene or 1, 3, 4-oxadiazol ligand, plays a significant role in the HOMO-LUMO energy gap.

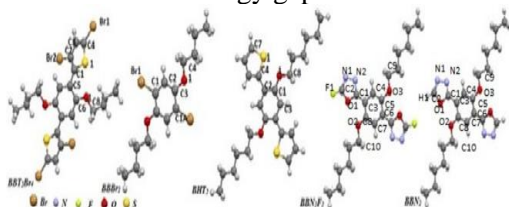


Figure.1. The schematic structures of the studied diodes

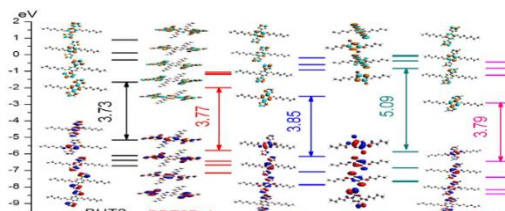


Figure.2. Frontier molecular orbital energy level diagram of diodes

Table.1. Optimized bond distances (Å) and bond angles (°) for the diodes with B3lyp 6-31G (d, P).

BBBr ₂					
Bond length (Å)		Bond angles		Dihedral angle	
Br ₁ -C ₁	1.905 (1.900)	C2-C1-Br1	118.8 (118.7)	C4-O1-C3-C2	2.26 (3.3)
O1-C ₃	1.358 (1.366)	O1-C3-C1A	117.9 (117.7)		
O1-C4	1.428 (1.441)	O1-C3-C2	124.4 (124.3)		
BHT ₂					
Bond length (Å)		Bond angles		Dihedral angle	
S1-C7	1.730 (1.707)	C7-S1-C4	92.10 (92.24)	C4-C2-C1-O1	2.50
S1-C4	1.759 (1.738)	C1-O1-C8	119.50 (118.42)		
O1-C1	1.367 (1.369)	O1-C1-C3	123.30 (123.50)		
O1-C8	1.426 (1.432)	C2-C4-S1	124.10 (123.82)		
BBT ₂ Br ₄					
Bond length (Å)		Bond angles		Dihedral angle	
Br1-C4A	1.883 (1.874)	C4-S1-C1	91.80 (91.70)	C6-C5-C1-S1	41.49(41.43)
Br2-C2	1.905 (1.886)	C6-O1-C8	119.10 (117.94)		
S1-C4	1.733(1.716)	C2-C1-S1	108.70 (109.12)		
S1-C1	1.743 (1.738)	C5-C1-S1	121.31(121.31)		

Table.2. Optimized bond distances (Å) and bond angles (°) for the new diodes with B3lyp 6-31G (d,P).

BBN ₂					
Bond length (Å)		Bond angles		Dihedral angle	
N1-N2	1.391	C1-O1-C2	102.37	O1-C1-C3-C8	0.17
N1- C2	1.292	O1-C1-C3	122.33		
N2- C1	1.307	C1-C3-C8	124.33	C1-C3-C8-O2	0.03
O1- C1	1.366	O2-C8-C3	117.72		
O1- C2	1.356	O2-C8-C7	123.61		
H1- C2	1.078				
C1- C3	1.460				
O2- C8	1.358				
O2- C10	1.431				
BBN ₂ F ₂					
Bond length (Å)		Bond angles		Dihedral angle	
N1-N2	1.391	C1-O1-C2	102.37	O1-C1-C3-C8	0.15
N1- C2	1.292	O1-C1-C3	122.33		
N2- C1	1.307	C1-C3-C8	124.33	C1-C3-C8-O2	0.05
O1- C1	1.366	O2-C8-C3	117.72		
O1- C2	1.356	O2-C8-C7	123.61		
H1- C2	1.078				
C1- C3	1.460				

O2- C8	1.358				
O2- C10	1.431				

Reactivity indices and molecular electrostatic potential MEP: The global hardness η measures the stability of a system in terms of resistance to electron transfer and the chemical potential μ characterizes the escaping tendency of electrons from the equilibrium system. Each system's η and μ are calculated from the ε_{HOMO} and the ε_{LUMO} with the relations:

$$\eta = \frac{1}{2}(\varepsilon_{LUMO} - \varepsilon_{HOMO}) \quad (1)$$

$$\mu = \frac{1}{2}(\varepsilon_{LUMO} + \varepsilon_{HOMO}) \quad (2)$$

The electrophilicity ω introduced by Parr. Measures the ability of a molecule to accept electrons from the surroundings. It is calculated with the relation:

$$\omega = \frac{\mu^2}{2\eta} \quad (3)$$

In Table.3, we display the computed values of the electronic chemical potential μ , chemical hardness η , and electrophilicity index ω of diodes, which appeared of BBN_2 and BBN_2F_2 the most electronegative molecules they are strongly activated electrophilic substitution. That indicates the power of 1, 3, 4-oxadiazol in a molecule to attract electron to itself. Inspection of Table.3, reveals clearly that the η values of compounds BHT_2 , BBT_2Br_4 , BBN_2F_2 and BBN_2 are nearly similar, but of $BBBr_2$ the hardness η value is higher than of those compounds BHT_2 , BBT_2Br_4 , BBN_2F_2 and BBN_2 , indicating that the stabilities of compounds BHT_2 , BBT_2Br_4 , BBN_2F_2 and BBN_2 are equal; which a small energy gap is favorable for soft molecules, of $BBBr_2$ is the most stability; which a large energy gap is favorable for hard molecules. The results confirmed by maps of electrostatic potential for the diodes see Fig.3, around a molecule is given more information to show reactive sites for electrophilic and nucleophilic attack, The color code of these maps is the range between $-1.055e^{-2}eV$ (deepest red) to $1.055e^{-2}eV$ (deepest blue); the positive (blue color) regions of MEP are related to electrophilic reactivity and the negative (red color) regions to nucleophilic reactivity. Furthermore, the partial negative charges are on the thiophene ring, while the partial positive charges are on the 1, 3, 4-oxadiazol ring; from these results, it can be inferred that the 1, 3, 4-oxadiazol ring indicates the strongest electrophilic compounds and thiophene ring the strongest nucleophilic compounds.

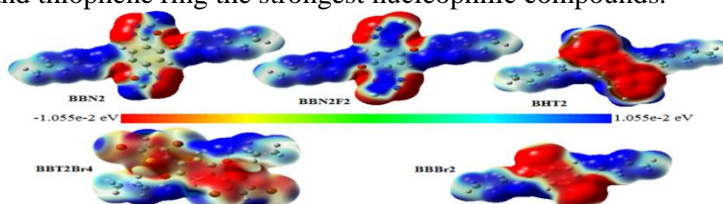


Figure.3. Maps of electrostatic potential for the new diodes

Table.3. Global reactivity descriptors: chemical potential (μ , eV), chemical hardness (η , eV) and electrophilicity index (ω)

	$BBBr_2$	BHT_2	BBT_2Br_4	BBN_2	BBN_2F_2
μ	-3.323	-3.075	-3.539	-3.878	-4.066
η	2.549	1.863	1.886	1.925	1.896
ω	2.160	2.530	3.320	3.901	4.360

Topological study of electron density: The topological analysis of the electron density ρ based on Bader's AIM theory; allows a quantitative description of different intermolecular and intramolecular interactions. The critical point (CP) in the electron density, and this determines the positions of extrema in ρ (maxima, minima, or saddle points), which there are four types of stable CP: (3, -3), nuclear critical; (3, -1) bond critical point (BCP); (3, + 1) ring critical point; (3, + 3) cage critical point, a better description can be based on the topological properties of electron density ρ , Laplacian $\nabla^2\rho$, the kinetic energy density $G(r)$ and the local electronic energy density H at bond critical points BCP precisely, values of $\rho < 0.07$, $\nabla^2\rho > 0$, $V/G < 1$, and H has a positive value are indicative of the closed-shell interactions such as ionic, hydrogen bonding. The results of calculations resumed in Table.4, reveal the characteristics of the closed-shell interactions at BCP of BHT_2 in thiophene ring according experimental data located at $C5 \cdots H5 \cdots C_{g1}$ (2.88 Å), $C5-C_{g1}$ (1.80 Å) and $C5-H5 \cdots C_{g1}$ (169°); C_{g1} is the centre of the S1,C4-C7 thiophene ring. A strong covalent bond are detected in BHT_2 , this is probably the result of covalent contact between thiophene and benzene ring in H1-H5 (2.03 Å).

From the mulliken charge calculation, the positive and negative charge separation between oxygen (-0.539) and sulfur (+0.342), that indicates the O-S bond (2.74 Å) is predominantly ionic, for BHT_2 and BBT_2Br_4 , also we found nearly the same negative charge between oxygen (-0.542) on the alkyloxy groups and oxygen (-0.459) on the 1,3,4-oxadiazol ring groups that indicates the O-O bond (2.63 Å) is predominantly covalent, for BBN_2 and BBN_2F_2 ,

of compound BBT_2Br_4 contain hydrogen bond located at $\text{C7-H7}\dots\text{Br2}$ in good agreement with experimental data, $\text{H7}\dots\text{Br2}$ 2.78 Å (2.80 Å) and $\text{C7-H7}\dots\text{Br2}$ 114° (114°), the bond critical point (BCP) are shown in Fig.4.

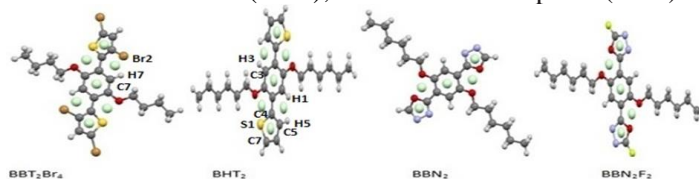


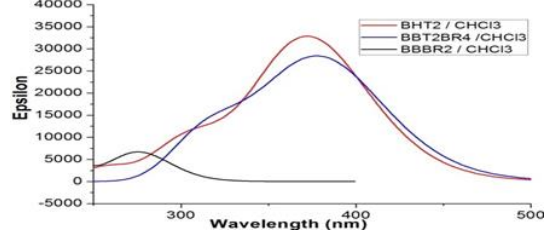
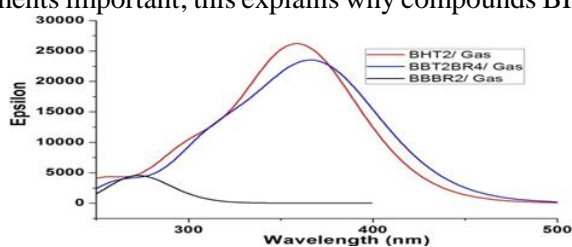
Figure.4. Representative bond critical point BCP and RCP (green) of the studied diodes

Table.4. QTAIM calculated values of: electron density (ρ), Laplacian ($\nabla^2\rho$), the kinetic energy density $G(r)$, and the local electronic energy density (H)

		$\rho(r)$	$\nabla^2\rho(r)$	V/G	$H(r)$
BBT_2Br_4	Thiophene ring RCP	0.0411	0.2297	0.9464	0.0028
	Benzene ring RCP	0.0231	0.1427	0.8492	0.0047
	O-S BCP	0.0149	0.0587	0.8292	0.0021
	Br2-H7 BCP	0.0119	0.0377	0.8405	0.0013
BHT_2	Thiophene ring RCP	0.0413	0.2297	0.9482	0.0028
	Benzene ring RCP	0.0231	0.1427	0.8491	0.0047
	O-S BCP	0.0186	0.0727	0.8642	0.0022
	H1-H5 BCP	0.0127	0.0485	0.8083	0.0020
BBN_2	1,3,4-oxadiazole ring RCP	0.0629	0.4154	0.9953	0.0005
	Benzene ring RCP	0.0231	0.1423	0.8486	0.0047
	O-O BCP	0.0126	0.0661	0.7570	0.0032
BBN_2F_2	1,3,4-oxadiazole ring RCP	0.0629	0.4154	0.9953	0.0005
	Benzene ring RCP	0.0231	0.1423	0.8486	0.0047
	O-O BCP	0.0126	0.0661	0.7570	0.0032

Photo physical properties:

Absorption and emission properties: Time dependent density functional theory TDDFT has become one of the most prominent and most widely used approaches for the calculation of excited state properties of medium to large molecular systems. The calculated absorption wavelengths of BHT_2 and BBT_2Br_4 are shown in Table.5, 6. To consider the functional effects and test the different functional method, TD/B3lyp with 6.31G (d, p) basis set reveal good agreement with the experimental data. However, the results obtained from the B3LYP with 6.31G(d, p) method are much closer to the experimental values than these of the CAM-B3LYP the main contribution of the corresponding maximal absorption corresponds to the promotion of one electron from the HOMO to the LUMO, Which is a $\pi\text{-}\pi^*$ transition; it is interesting to note that the contribution of the alkyloxy groups to the electronic absorption is vanishingly small, Therefore, the absorption spectra in BHT_2 and BBT_2Br_4 , are simulated in gas and solvent phase CHCl_3 , the main band located in near visible region with broad and strong absorption characteristics in agreement with $\text{H}\rightarrow\text{L}$ transition; which show that appropriate consideration of solvent effects is not necessary to explain the experimental phenomena see Fig.5 and Table.7. The oscillator strength f of the studied compounds on absorption and emission spectra increases in the following order $\text{BBBr}_2 < \text{BBN}_2 < \text{BBN}_2\text{F}_2 < \text{BBT}_2\text{Br}_4 < \text{BHT}_2$, this means those compounds BHT_2 and BBT_2Br_4 have a greater emission than those compounds BBBr_2 , BBN_2 and BBN_2F_2 , and Compounds BHT_2 and BBT_2Br_4 are shown red shift emission, which are in agreement with $\text{L}\rightarrow\text{H}$ transition see Table.8, the maximum emission show at 462nm, 335nm for molecules BBN_2 and BBN_2F_2 respectively, which are the most intense band and agree well $\text{L}+1\rightarrow\text{H}$ transition, $\text{L}\rightarrow\text{H}-1$ transition respectively. On the other hand, for BBBr_2 , the maximum emission show at 506 nm in agreement with $\text{H}-1\rightarrow\text{L}$ transition, we can say that the emission peaks of the studied compounds exhibit a hypsochromic shift with increasing the 1,3,4-oxadiazol ring; indicates the strongest electrophilic compounds and the dipole moments negligible, but the emission peaks of BHT_2 and BBT_2Br_4 exhibit bathochromic shift with increasing the thiophene ring; the strongest nucleophilic compounds and the dipole moments important; this explains why compounds BHT_2 and BBT_2Br_4 have a larger emissive and stokes shift (Fig.5).



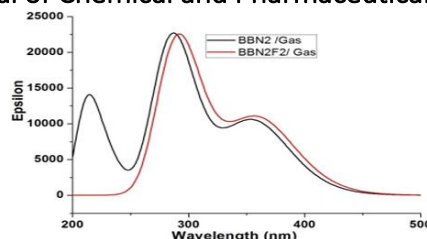
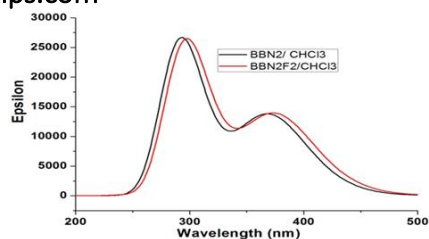


Figure.5. Absorption spectra obtained by TDDFT methods for these diodes, together in gas and solvent (CHCl_3) phase

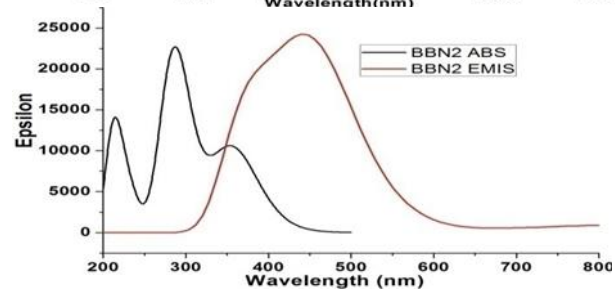
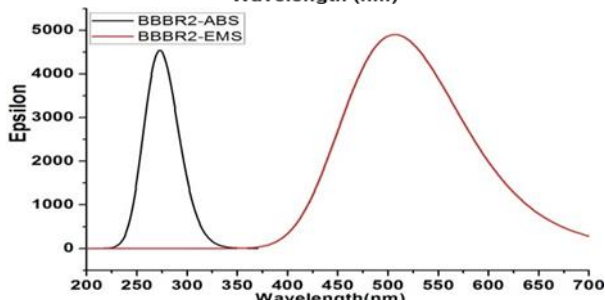
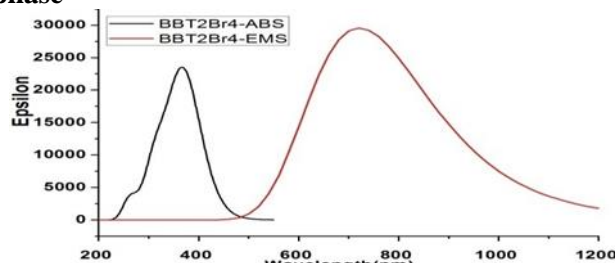
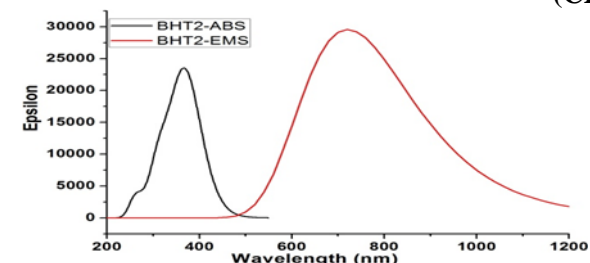


Figure.6. Theoretical absorption spectra (black line) and emission spectra (red line) of diodes

Table.5. A comparison of computed absorption maxima ($\lambda_{\text{max}}^{\text{abs}} = \text{nm}$), oscillator strengths (f) at various levels with experimentally reported value of BHT₂

Method	Cam-B3lyp	B3lyp	Cam-B3lyp	B3lyp	exp
	LANL2DZ		6-31G (d, P)		
λ (nm)	332	377	328	360	361
	276	317	272	302	305

Table.6. A comparison of computed absorption maxima ($\lambda_{\text{max}}^{\text{abs}} = \text{nm}$), at various levels with experimentally reported value of BHT₂ and BBT₂Br₄

Method		B3lyp LANL2DZ		B3lyp 6-31G (d, P)		$\lambda_{\text{max}}^{\text{Exp}}$ (nm)
BHT ₂		Gas	solvent	Gas	solvent	
	λ (nm)	377	403	360	373	361
	λ (nm)	317	325	302	306	305
BBT ₂ Br ₄	λ (nm)	372	386	370	381	344
		317	322	315	319	297

Table.7. Absorption spectra obtained by TDDFT methods for these diodes, together in gas and solvent (CHCl_3) phase

Diodes	Absorption λ_{max} (nm)		gas			CHCl_3		
			λ	E	f	λ	E	f
BBBr ₂	H \rightarrow L	ICT	273	4.543	0.111	276	4.495	0.161
	H \rightarrow L+2	ICT	229	5.404	0.000	229	5.416	0.000
	H \rightarrow L+3	ICT	273	4.533	0.000	230	5.381	0.000
	H-1 \rightarrow L	ICT	211	5.869	0.000	209	5.914	0.000
BHT ₂	H \rightarrow L	ICT	360	3.431	0.631	373	3.323	0.800
	H-1 \rightarrow L	ICT	302	4.099	0.224	306	4.041	0.259
	H-1 \rightarrow L+1	CT	264	4.683	0.000	269	4.600	0.000
	H-2 \rightarrow L	ICT	284	4.356	0.000	285	4.349	0.000
BBT ₂ Br ₄	H \rightarrow L	ICT	370	3.343	0.545	381	3.253	0.672
	H-1 \rightarrow L	ICT	315	3.926	0.260	319	3.884	0.316

	H-3→L	ICT	265	4.649	0.042	267	4.595	0.040
	H→L+4	ICT	263	4.707	0.020	265	4.649	0.004
BBN ₂	H→L	ICT	356	3.481	0.251	369	3.335	0.348
	H-1→L	ICT	287	4.321	0.556	292	4.233	0.656
	H→L+1	CT	242	5.114	0.000	251	4.926	0.000
BBN ₂ F ₂	H→L	ICT	360	3.440	0.260	375	3.300	0.338
	H-1→L	ICT	291	4.250	0.550	297	4.160	0.651
	H→L+1	CT	255	4.850	0.000	256	4.829	0.000

Table.8. Absorption and emission of diodes calculated by TD-DFT in gas phase

Diodes	E _{Abs} (eV)	λ_{max}^{Abs} (nm)	<i>f</i>	E _{Ems} (eV)	λ_{max}^{Ems} (nm)	<i>f</i>	$\Delta\lambda^{gaz}$
BHT ₂	3.44	360	0.63	1.74	711	1.29	351
BBT ₂ Br ₄	3.34	370	0.54	1.69	731	0.95	361
BBBr ₂	4.54	273	0.11	2.44	506	0.12	233
BBN ₂	4.32	287	0.56	2.68	462	0.41	175
BBN ₂ F ₂	4.25	291	0.54	3.70	355	0.55	44

4. CONCLUSION

The quantum calculations were performed on a series of organic diode by means of the DFT and TDDFT methods. The results reveal that the alkyloxy group has minor effect on electronic and topologic structural parameters in ground and excited state geometries. The lower LUMO energy for BBN₂ and BBN₂F₂ are favorable for electron transport. On the other hand, the higher HOMO energy for BHT₂ and BBT₂Br₄ are also favorable for hole transport. Analysis of intramolecular bonds indicates the presence of ionic and hydrogen interactions. The maps of electrostatic potential shows the nucleophilic character in the diode thiophene ligand and the electrophilic in the diode contained the 1, 3, 4-oxadiazole group. The emission spectra in BHT₂ and BBT₂Br₄ are given red shift emission with large stokes coefficient, the diodes contained 1, 3, 4-oxadiazole groups in BBN₂ and BBN₂F₂ are shown hypsochromic shift emission.

REFERENCES

- Antonio Sanchez-Coronilla, Jesus S, Anchez M, Arquez, David Zorrilla, Elisa Martin I, Desiree de los Santos M, Javier Navas, Concha Fernandez-Lorenzo, Rodrigo Alcantara and Joaquin Martin-Calleja, Convergent study of Ru–ligand interactions through QTAIM, ELF, NBO molecular descriptors and TDDFT analysis of organometallic dyes, *Molecular Physics*, 112, 2014, 2063–2077.
- Bader R.F.W, Can There Be More Than a Single Definition of an Atom in a Molecule, *Canadian Journal of Chemistry*, 77, 1999, 86 – 93.
- Badlo M.A, Thompson M.E & Forrest S.R, High-efficiency fluorescent organic light-emitting devices using a phosphorescent sensitizer *Nature*, 403, 2000, 750-753.
- Basem Fares Ali, Rawhi Al-Far H and Salim Haddad F, 3-Ammoniopyridinium tetra bromido mercurate (II) monohydrate, *Acta Cryst*, E64, 2008, 751-752.
- Bernhard Schlegel H, Optimization of equilibrium geometries and transition structures, *Journal of Computational Chemistry*, 3, 1982, 214–218.
- Chermette H, Chemical reactivity indexes in density functional theory, *J. Comput. Chem*, 20, 1999, 129-154.
- Chin Hoong Teh, Muhammad Mat Salleh, Mohamed Ibrahim Mohamed Tahir, Rusli Daik, Mohammad B, Kassim, 1,4-Dibromo-2,5-dibutoxybenzene, *Acta Cryst*, E68, 2012, o2683.
- Chin Hoong Teh, Muhammad Mat Salleh, Mohamed Ibrahim Mohamed Tahir, Rusli Daik, Mohammad B. Kassim, 2,2-[2,5-Bis(hexyloxy)-1,4-phenylene]dithiophen, *Acta Cryst*, E68, 2012, o1976.
- Chin Hoong Teh, Rusli Daik, Muhammad Mat Salleh, Mohamed Ibrahim Mohamed Tahir, Mohammad B, Kassim, 3,5-Dibromo-2-[2,5-dibutoxy-4-(3,5-dibromothiophen-2-yl)phenyl]thiophene, *Acta Cryst*, E67, 2011, o3183.
- Facchetti A, Semiconductors for organic transistors, *Mater Today*, 10, 2007, 28-37.
- Forrest S R, Thompson M E, Introduction, organic electronics and optoelectronics, *Chem Rev*, 107, 2007, 923-925.
- Frisch M.J, Trucks G.W, Schlegel H.B, Scuseria Gaussian G.E, Inc, Wallingford CT, 2009.
- Fuyu Sun, Ruifa Jin, DFT and TD-DFT study on the optical and electronic properties of derivatives of 1,4-bis (2-substituted-1,3,4-oxadiazole)benzene, *Arabian Journal of Chemistry*, 11, 2013, 037.

Geerlings P, De Proft F, and Langenaeker W, Conceptual Density Functional Theory, *Chem. Rev*, 103, 2003, 1793–1874.

Gigli G, Barbarella G, Favaretto L, Cacialli F, R Cingolani R, High-efficiency oligothiophene-based light-emitting diodes, *Applied physics letters*, 75 , 1999, 439-441.

Gogoi U, Guha AK, AK Phukan AK, Nature of intramolecular metal–metal interactions in supported group 4–group 9 and group 6–group 9 heterobimetallic complexes, a combined density functional theory and topological study, *Organometallics*, 30, 2011, 5991-6002.

Gokhan Gece and Semra Bilgic, Molecular-Level Understanding of the Inhibition Efficiency of Some Inhibitors of Zinc Corrosion by Quantum Chemical Approach, *Ind. Eng. Chem. Res*, 51, 2012, 14115–14120.

Jin S.H, Kim M.Y, Kim J.Y, Lee K, Gal Y.S, High- efficiency poly (p-phenylene vinylene)-based copolymers containing an oxadiazole pendant group for light emitting diodes, *J. Am. Chem. Soc*, 126, 2004, 2474–2480.

John Perdew P, Kieron Burke and Matthias Ernzerhof, Generalized Gradient Approximation Made Simple, *Phys. Rev. Lett*, 77, 1996, 3865.

John Perdew P, Kieron Burke, and Matthias Ernzerhof, Generalized Gradient Approximation Made Simple, *Phys. Rev. Lett*, 78, 1997, 1396.

Leriche P, Frere P, Cravino A, Aleveque O, Roncali J, Molecular engineering of the internal charge transfer in thiophene triphenyl amine hybrid, *J Org Chem*, 72, 2007, 8332-8336.

Lin Y, Fan H, Li Y, Zhan X, Thiazole-based organic semiconductors for organic electronics, *Adv Mater*, 24, 2012, 3087-3106.

Liu L.L, Pan X.M, Zheng W, Cui L.L, Yang G.C, Su Z.M, Wang R.S, The modulation of electronic and optical properties of OXD-X through introduction of the electron-withdrawing groups: A DFT study, *Journal of Molecular Graphics and Modelling*, 28, 2010, 427–434.

Manna D, Ghanty TK, Complexation behavior of trivalent actinides and lanthanides with 1, 10-phenanthroline-2, 9-dicarboxylic acid based ligands, insight from density functional theory, *Physical Chemistry Chemical Physics*, 14, 2012, 11060-11069.

Ralph G, Pearson, The electronic chemical potential and chemical hardness, *Journal of Molecular Structure, Theochem*, 255, 1992, 261-270.

Robert Parr G, Laszlo Szentpaly V and Shubin Liu , Electrophilicity Index, *J. Am. Chem. Soc*, 121 , 1999, 1922–1924.

Robert Parr G, Ralph Pearson G, Absolute hardness: companion parameter to absolute electronegativity, *J. Am. Chem. Soc.*, 105, 1983, 7512–7516.

Tang C.W, Vanslyke S.A, Organic electroluminescent diodes, *Appl. Phys*, 51, 1987, 913.

Tevelde G, Bickelhaupt F.M, Van Gisbergen S.J.A, Fonseca Guerra C, Baerends E.J, Snijders J.G and Ziegler T, Chemistry with ADF, *Journal of Computational Chemistry*, 22, 2001, 931.

Van Lenthe E, Ehlers A.E and Baerends E.J, Geometry optimization in the Zero Order Regular Approximation for relativistic effects, *Journal of Chemical Physics*, 110, 1999, 8943.

Wang C.S, Jung G.Y, Hua Y.L, Pearson C, Bryce M.R, Petty M.C, Batsanov A.S, Goeta A.E, Howard J.A.K, An efficient pyridine-and oxadiazole- containing hole-blocking material for organic light-emitting diodes, synthesis, crystal structure and device performance, *Chem. Mater*, 13, 2001, 1167–1173.

Wang J.F, Jabbour G.E, Mash E.A, Anderson J, Zhang Y, Lee P.A, Armstrong N.R, Peyghambarian N, Kippelen B, Oxadiazole Metal Complex for Organic Light-Emitting Diodes, *Advanced Materials*, 11, 1999, 1266–1269.